Analysis of influence of land use/land cover changes on the land surface temperature of Växjö Municipality, Sweden

Aarthi Aishwarya Devendran
Post-doctoral Researcher
Linnaeus University
Växjö
Sweden
aarthi.devendran@lnu.se

Brijesh Mainali
Associate Senior Lecturer
Linnaeus University
Växjö
Sweden
brijesh.mainali@lnu.se

Krushna Mahapatra
Professor
Linnaeus University
Växjö
Sweden
krushna.mahapatra@lnu.se

Keywords

climate change, urban model, cellular automata, Växjö Municipality, land use

Abstract

Human activities are responsible for almost 75 % of the land cover changes depleting the natural resources globally. These land cover changes with decreasing vegetation and water bodies increase the heat emissions from the land surface thereby influencing the climate changes regionally and globally. This paper highlights the interaction and interlinkages between the land use changes due to human activities (Sustainable Development Goal (SDG) 15) and its consequences on climate changes (SDG 13) using spatial analysis techniques. In this context, the climate change of Växjö Municipality, Sweden resulting from the urban development is demonstrated through LST (Land Surface Temperature), NDVI (Normalised Difference Vegetation Index), NDBI (Normalised Difference Built-Up Index) and land cover changes as indicators through Landsat 8 data of 2014, 2016, 2018 and 2020. The land cover maps prepared through Support Vector Machine algorithm indicate that the area of built-up had doubled during the study periods with decreasing open lands. The LST maps prepared from the thermal bands of the Landsat 8 data showed an increase in the mean surface temperature from 7.3 °C to 11.1 °C between 2014 and 2020. The study also aims to study the seasonal variations in the relationship between LST, NDVI and NDBI by making use of Landsat 8 dataset acquired during the spring, summer, and autumn seasons of 2019. Results suggest a strong positive relationship between LST and NDBI (0.74) whereas a negative relationship is found associated between LST and NDVI (0.65) and between NBDI and NDVI (0.71). Further the land cover and LST maps of 2014 and 2020 are used in the simulation of urban and LST maps of 2050 through Cellular Automata model to highlight the impact of urban development on the climate changes of Växjö Municipality. The simulation result predicts that the built-up area of 2020 might quadruple in 2050. The simulation analysis also predicted an increase in LST with increasing urbanization in the study region. This study emphasises that the land cover changes in the process of urban development is also a contributing factor for climate change in the study region which is evident from the increase in mean surface temperature (3.8 °C) from 2014 to 2020.

Introduction

Increased urbanization, resulting in rapid expansion of cities and metropolitan regions is one of the most important drivers of climatic changes globally. Three main factors influence the urbanization of a region including the natural increase in population which varies according to a region, migration of people to cities and gradual increase in the size of the existing cities (United Nations, 2018). By 2050, the global population is expected to reach 9.7 billion with 68 % of the population expected to live in urban areas (Sun *et al.*, 2020). This rapid increase in the urbanization leads to depletion of natural resources, change in the climatic conditions both at regional and global level and degradation of quality of living of humans. Rapid urbanization results in the permanent conversion of large areas of cropland and natural vegetation to impervious surfaces thereby greatly modifying the land surface properties and land-atmosphere interactions (Qiao *et al.*, 2020). One of the impacts of rapid ur-

banization and urban expansion is the increased Land Surface Temperature (LST) of a region. Globally, deforestation, due to rapid urbanization, has possibly contributed to the increased LST and increased greenhouse gas emissions thereby impacting the climate change (Aik *et al*., 2020). Researches on estimating the LST as an indicator for climate and ecological changes are widely reported. In countries located in the arctic cold zone including Sweden, the resources of glacial snow and frozen soil in the region are relatively rich, which is very important for the balance and stability of the ecological environment in the region. A large continuous increase in LST is an important threat to the ecological environment in this region and must be considered (Yan *et al*., 2020). Changes in the LST of a region are caused by the anthropogenic activities within the urban areas and thus it becomes crucial to monitor the effect of change in land use/land cover on LST to implement appropriate climatic mitigation measures in the region. Although the terms land cover and land use are often used interchangeably, their actual meanings are quite distinct. It is important to distinguish the difference between land cover and land use, and the information that can be ascertained from them. The properties measured with remote sensing techniques relate to land cover, from which land use can be inferred, particularly with ancillary data or a priori knowledge. Land cover refers to the surface cover on the ground, whether vegetation, urban infrastructure, water, bare soil or other. Identifying, delineating, and mapping the land cover is important for global monitoring studies, resource management, and planning activities. Land use refers to the purpose the land serves, for example, recreation, wildlife habitat, or agriculture. Spatial analysis based on temporal dataset is required to identify the land use category of a land and to analyze the land use changes from year to year.

With the availability of remote sensing based high resolution, multi-temporal satellite images along with the advancements in GIS (Geographic Information System) based spatial analysis techniques, studies on analyzing the effects of urban growth on the surface temperature of a region is gaining importance recently. Land cover is the pattern of ecological resources and human activities dominating the different areas of Earth's surface (Meyer and Turner, 1994). It is a critical data essential for many environmental monitoring and natural resources management applications at local, regional, and global scales (Shi and Yang, 2015). Support Vector Machine (SVM) is a non–parametric classification method (Richards, 2013) belonging to the field of machine learning technique, which does not require prior knowledge of the statistical distribution of a dataset to be classified. In the recent times, SVM based classification techniques are gaining increasing attention in the field of remote sensing applications including land use/land cover classification due to their ability to minimize the classification errors and superior generalization characteristics, while solving the classification problems (Mathur and Foody, 2004).

Urban growth models have been developed and extensively adopted to study the urban sprawl and its impact on the ambient environment. These models can be employed in urban policy making or analyses of development scenarios (Li and Gong, 2016). Cellular Automata (CA) models are widely used to model the urban growth as CA based models are found to perform well in predicting the urban development closer to the reality than conventional mathematical models (Mubea *et al.,* 2014). A detailed review on urban growth models based on CA is given by Triantakonstantis and Mountrakis (2012).

Numerous studies on the estimation of LST using Landsat imageries are carried out in various countries (Meng *et al.,* 2019; Srivastava *et al.,* 2009; Qin and Karnieli, 2001). Mukherjee and Singh (2020) investigated the spatial and temporal changes in land use and patterns of vegetation and its impact on LST in two Indian cities. The study showed a negative correlation between Normalised Difference Vegetation Index (NDVI) and LST in the cities with increasing temperature of 2.13 °C per decade. The effects of changes in the landscape on the LST of Addis Ababa, Ethiopia were estimated using Landsat data (1986–2016) (Dissanayake *et al.,* 2019). The results of their study highlight that impervious areas dominate the study region which had major contribution in the increased LST which had increased approximately 4 °C during the study periods. The findings of their study could be useful for the decision makers to introduce sustainable landscape and urban planning in Addis Ababa.

According to the European Environment Agency (2021) the warmest year in Europe was 2014 with 2015 and 2016 closely joint second, and 2017 the fourth warmest year since 1850. The record high temperatures in 2014 were 35 to 80 times more likely because of anthropogenic climate change. This high warming has been reported particularly over southern Scandinavia. In this context, the objectives of the current study is to analyze the impact of changes in the land cover pattern on the LST of Växjö Municipality, Sweden between 2014 and 2020 using Landsat 8 dataset and to simulate the increasing urban growth and LST in 2050 through using CA-Markov model. The study also aims to study the seasonal variations in the relationship between LST, NDVI and Normalised Difference Built-Up Index (NDBI) of the study region using Landsat 8 data of 2019 through regression analysis technique.

Study Area

Växjö Municipality is the administrative, cultural, and industrial centre of Kronoberg County, and is located in the southern Sweden. The study area map of Växjö Municipality is shown in Figure 1. The municipality is spread over an area of 1,927 km² with a population of 94,274 as on March 2020. Växjö Municipality has a long-term and strategic environmental and climate work and has been called 'The Greenest City in Europe' since 2007.

Data and Methods

To simulate the urban growth and the LST of Växjö Municipality in 2050 and to identify the relationship between LST, NDVI and NDBI of the study region, the following datasets are used:

1. Landsat 8 data with 15-meter resolution acquired on 13th March 2014, 11th April 2016, 2nd April 2018 and 6th April 2020, available from United States Geological Survey (USGS) Earth Explorer (https://earthexplorer.usgs.gov/), are used in the preparation of land cover maps of the corresponding years.
2. Band 10 of Landsat 8 data with 100-meter resolution are used to derive the LST maps of the study region during the study periods.

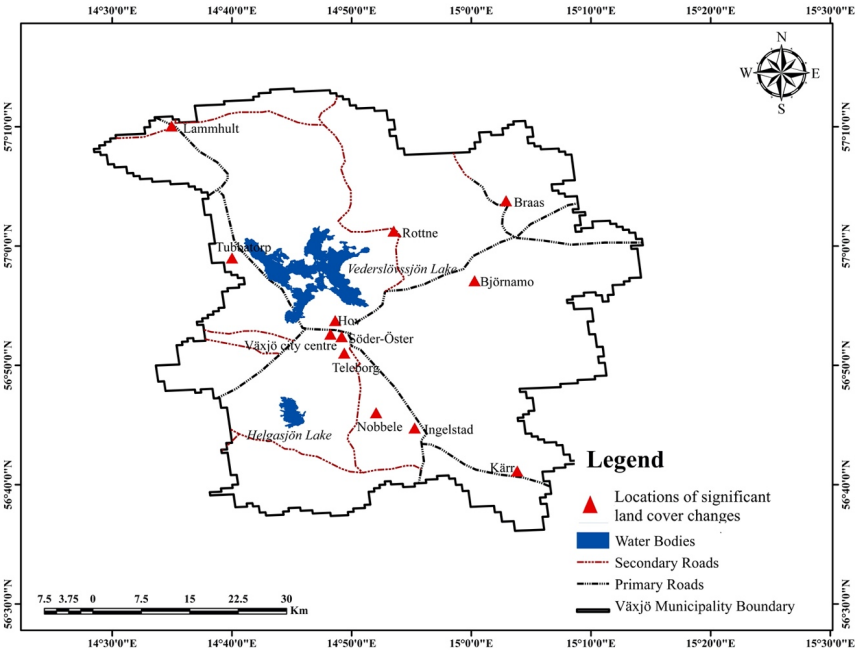

Figure 1. Map of the Study Region.

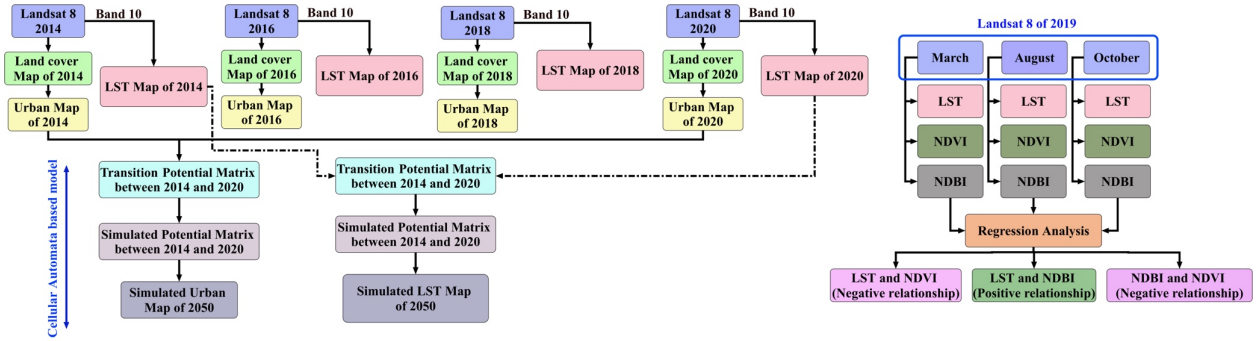

Figure 2. Methodology adopted in the study.

3. Bands 4, 5 and 6 with 30-metre resolution and Band 10 (100-metre resolution) of Landsat 8 are used in the derivation of NDVI, NDBI and LST during the months of March, August, and October of 2019.
4. Google Earth along with field information are used in the validation of land cover maps of the study region.

The methodology adopted for the current study is shown in Figure 2. The steps involved include the preparation of urban maps of 2014, 2016, 2018 and 2020 from the land cover maps derived from the Landsat 8 data of the study region. Using the observed urban maps of 2014 and 2020, urban map of 2050 is prepared through CA-Markov based simulation modeling technique. The Band 10 of Landsat 8 data is used in the estimation of LST maps of the region. The historical LST maps of the study region are used in the simulation of LST map of 2050 through CA-Markov model. Linear Regression analysis is carried out to study the seasonal variations in the relationships between LST, NDVI and NDBI of the study region in 2019.

URBAN MAP

The land cover maps of the study region, prepared through SVM technique of supervised classification, contain four categories including Built-Up, Vegetation, Water body and Open lands. The current study focuses on simulating the urban expansion of Växjö Municipality in the future and thus the land cover maps are converted into 'Urban Maps' which contain only binary categories: 'Built-Up' and 'Non-Built-Up'. The vegetation, water body, open lands categories were combined into a single category as 'Non-Built-Up'. Thus, from the land cover maps the urban maps of the study region are prepared for the years 2014, 2016, 2018 and 2020.

LAND SURFACE TEMPERATURE MAP

The estimation of LST using Landsat 8 data involves the following steps.

Calculation of TOA (Top Of Atmospheric) spectral radiance

The first step towards the estimation of LST is the calculation of TOA which is calculated using Equation 1.

$$TOA = M_L * Q_{CAL} + A_L \quad (1)$$

where,
M_L is the band specific multiplicative rescaling factor
Q_{CAL} corresponds to Band 10 of Landsat 8
A_L is the band specific additive rescaling factor

Conversion of TOA to Brightness Temperature (BT)

The spectral radiance is converted to BT as shown in Equation 2.

$$BT = \frac{K_2}{\ln\left(\left(\frac{K_1}{TOA}\right) + 1\right)} - 273.15 \quad (2)$$

where, K_1 and K_2 are the band specific thermal conversion constants. To obtain the brightness temperature value in degree Celsius, Equation 2 is adjusted by adding the absolute zero (-273.15) value.

Calculation of NDVI

In the process of estimation of LST, the calculation of NDVI is important. The amount of vegetation present is an important factor in estimating the LST, and NDVI can be used to infer the general vegetation condition of a study region (Mancino *et al.,* 2020). NDVI, a dimensionless value, is calculated by making use of the red and near-infrared bands of the Landsat 8 data.

$$NDVI = \frac{\text{Band 5} - \text{Band 4}}{\text{Band 5} + \text{Band 4}} \quad (3)$$

Calculation of Proportion of Vegetation (P_V)

From the NDVI, P_V is calculated using Equation 4

$$PV = \left(\frac{NDVI - NDVI_{Min}}{NDVI_{Max} - NDVI_{Min}}\right)^2 \quad (4)$$

where, $NDVI_{Min}$ and $NDVI_{Max}$ are the minimum and maximum values of NDVI.

Emissivity calculation

$$\varepsilon = 0.004 * P_V + 0.986 \quad (5)$$

where, ε is the land surface emissivity and 0.986 is the corrective value.

Estimation of Land Surface Temperature

The final step involves the retrieval of LST using Equation 6.

$$LST = \left(\frac{B_T}{1 + \left(0.00115 * \frac{B_T}{1.4388}\right) * ln(\varepsilon)}\right) \quad (6)$$

SIMULATION MODELING TECHNIQUE

The simulation of built-up and LST in 2050 is carried out through CA-Markov model (Aburas *et al.,* 2021; Nasehi *et al.,* 2019).

Urban Simulation

The urban maps of the year 2014 (t_1) and 2020 (t_2) are used in simulating the urban growth of the study region in 2050 (t_3). Traditional CA (TCA) model is implemented in an ArcGIS environment making use of the historical urban maps and with a 3×3 urban neighbourhood. Based on the transition potential matrix (TPM) between t_1 and t_2, the TPM between t_2 and t_3 is calculated which highlights the expected number of built-up and non-built-up pixels in 2050 based on CA-Markov model (Aarthi and Gnanappazham, 2018). (See Figure 2.)

Land Surface Temperature Simulation

The band 10 data of Landsat 8 is used in the estimation of LST of the study region during the spring of 2014, 2016, 2018 and 2020. The LST maps are further reclassified into four categories (0–14 °C; 14–20 °C; 20–24 °C; 24–39 °C). Using these reclassified LST maps and the urban maps of 2014 and 2020 the LST of the study region in the spring of 2050 is simulated using CA-Markov model (Tariq and Shu, 2020) in an ArcGIS environment (Figure 2).

RELATIONSHIP BETWEEN LST, NDVI AND NDBI

The relationship of LST with NDVI and NDBI might vary dynamically with the changes in the land cover patterns of the region and on the seasonal conditions during which the satellite image is acquired (Yang *et al.,* 2020). In the current study, to study the influence of changes in the seasons on the relationship between LST, NDVI and NDBI, Landsat 8 data acquired during Spring (March), Summer (August) and Autumn (October) of 2019 are analyzed through regression technique where NDVI and NDBI was considered as the independent variable and LST as the dependent variable as LST is found to be influenced by changes in the vegetation and built-up (Figure 2) (Govil *et al.,* 2020). Data pertaining to the winter season is not utilized in the analysis due to the non-availability of cloud-free dataset for the study region. The widely used index to study the condition of vegetation of a region (NDVI) (Guha *et al.,* 2018; Kumar and Shekhar, 2015) is implemented in the current study (as explained in Equation 3). NDVI is used to measure and map the density of green vegetation across a region. It is a ratio ranging between -1 and +1 values. Negative values of NDVI correspond to waterbodies whereas values closer to zero indicate barren areas of rock, sand or snow. Shrubs and grasslands exhibit lower positive NDVI values whereas higher positive values represent dense vegetation or tropical rain forest. NDBI is one of the most used indexes for the analysis of built-up areas. Using Landsat 8 data, NDBI can be calculated by making use of near-infra-red and short-wave infrared bands of Landsat 8 using Equation 7.

$$NDBI = \frac{\text{Band 6} - \text{Band 5}}{\text{Band 6} + \text{Band 5}} \quad (7)$$

Similar to NDVI, values of NDBI values also range between -1 and +1. Higher the positive values of NDBI, higher is the proportion of built-up and negative values of NDBI represent water bodies (Ogashawara and Bastos, 2012).

VALIDATION

Validation is an important process which enables the users to understand the accuracy of the land cover maps prepared through classification techniques. The most common way to express the classification accuracy is the preparation of Error Matrix also known as Confusion or Contingency matrix (Fang *et al.,* 2020). Different measures and statistics can be derived from the values in an error matrix. Overall Accuracy (OA) expressed in percent-

age is the ratio of the sum of diagonal values to the total number of cell counts in the matrix highlighting the percentage of testing samples that are classified correctly, whereas Kappa coefficient (*k*) takes the non-diagonal elements into account and is a measure of overall agreement of the error matrix (Rosenfield and Fitzpatrick-Lins, 1986).

Results and Discussions

LAND COVER MAP

Figure 3 explains the statistics of the land cover categories during the study period which reveal a gradual increase in the built-up area with decreasing open lands from 2014 and 2020. The area of built-up in 2014 was observed to be 28.46 km^2 which increased to 48.78 km^2, 57.37 km^2 and 64.34 km^2 in 2016, 2018 and 2020 respectively. The area of built-up of 2014 had doubled in 2020 with decreasing open lands during the study periods. The built-up is found to be concentrated around Teleborg, Söder-Öster, Växjö city centre, Hov in the study region (Figure 1). The validation results of SVM based land cover classification maps of 2014, 2016, 2018 and 2020 in terms of OA and *k* are shown in Table 1.

LAND SURFACE TEMPERATURE MAP

The LST of the study region estimated using the band 10 of the Landsat 8 data (Figure 2) showed considerable increase between the spring of 2014 and 2020 which is evident from the surface temperature maps of the region (Figure 4). The observed maximum surface temperature of the region increased almost 14 °C between 2014 and 2020 (24.91 °C in 2014 and 38.74 °C in 2020). It is seen that areas of built-up and open lands including Växjö

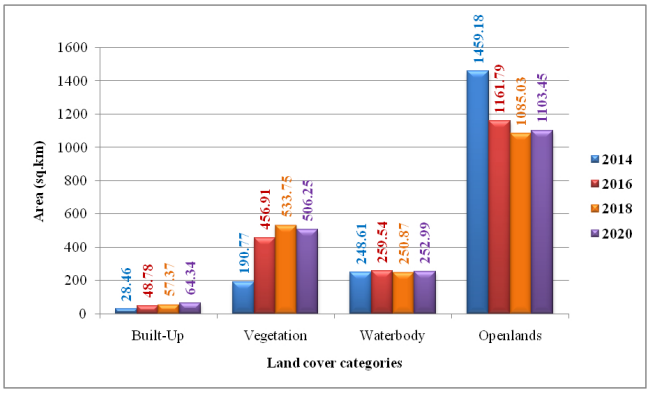

Figure 3. Statistics of the land cover categories of the study region.

Table 1. Accuracy Assessment of land cover maps prepared through SVM technique for the study region.

Study Periods / Accuracy Assessment	2014	2016	2018	2020
Overall Accuracy (%)	98.73	99.93	96.70	95.61
k value	0.98	0.99	0.95	0.95

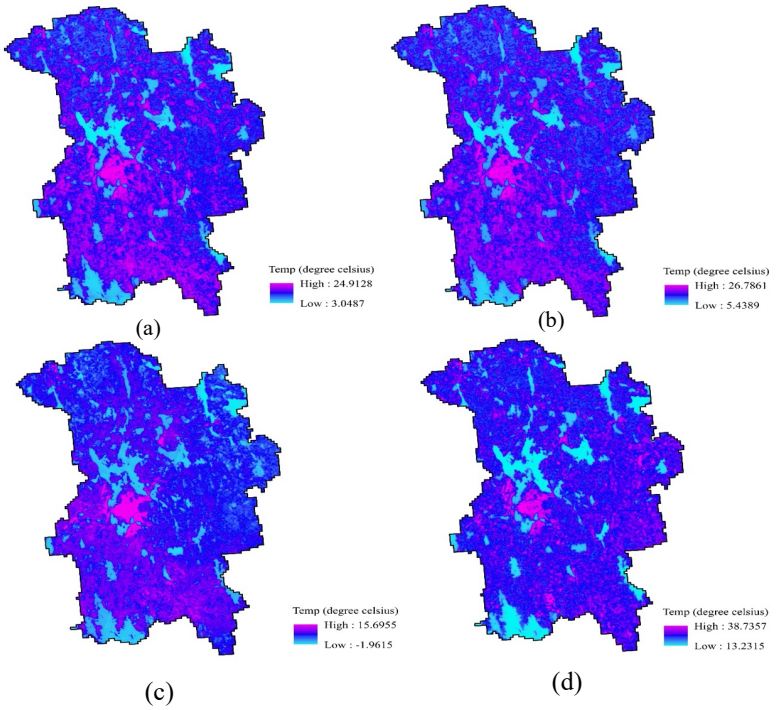

Figure 4. Land Surface Temperature Maps derived from Landsat 8 data acquired during the spring of (a) 2014; (b) 2016; (c) 2018; (d) 2020.

Table 2. Observed and Simulated transition probability matrix and its corresponding area between 2014 and 2020, 2020 and 2050.

	Observed Transition Probability between 2014 and 2020		Simulated transition probability between 2020 and 2050	
	Built-Up	Non-Built-Up	Built-Up	Non-Built-Up
Built-up	0.0148 (28.46 km²)	0	1 (64.33 km²)	0
Non-built-up	0.0186 (35.87 km²)	0.9666 (1862.69 km²)	0.1045 (194.66 km²)	0.8955 (1668.04 km²)

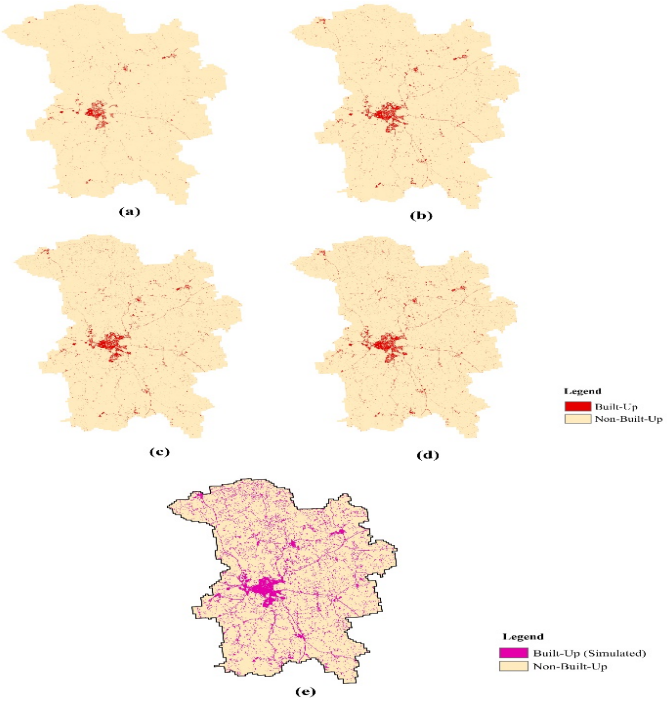

Figure 5. Urban Maps of the study region. Observed Urban Maps in (a) 2014; (b) 2016; (c) 2018; (d) 2020. Simulated Urban Map in (e) 2050.

city centre, Teleborg, Lammhult, Braas, Ingelstad and Nobbele exhibit higher surface temperature during the study periods. Waterbodies including Helgasjön lake, Vederslövssjön lake and vegetated areas in Björnamo, Kärr, Tubbatorp, Rottne show lowest surface temperature in the study region. This could be due to the fact that conventional human-made materials used in the urban environments such as pavements or roofing tend to absorb and emit more of the sun's heat compared to trees, vegetation, and other natural surfaces. This analysis highlights that an increase in built-up area by double, has possibly increased the mean LST by 3.8 °C between 2014 and 2020 in the study region.

SIMULATION TECHNIQUES

Simulated Urban Map of 2050

The simulated urban map of 2050 (Figure 5(e)) is prepared through CA-Markov model (Figure 2) based on the urban maps of 2014 and 2020 (Figure 5(a)–(d)). Based on the urban maps of 2014 and 2020, the observed TPM between 2014 and 2020 is calculated, which is further used in the calculation of the simulated TPM between 2020 and 2050. From Table 2, it is evident that 28.46 km² of built-up observed in 2014 remained as built-up in 2020. Further, 35.87 km² area of non-built-up observed in 2014 had converted to built-up in 2020 which makes the total observed built-up of 2020 to be 64.33 km². Based on this TPM between 2014 and 2020, it is expected that the built-up of 2020 (64.33 km²) might remain as built-up in 2050 and approximately 10.45 % of non-built-up of 2020 corresponding to an area of 194.66 km² is expected to be built-up in 2050. Thus, the simulated urban map of 2050 is expected to have 258.99 km² of built-up which is a quadruple of the built-up area in 2020.

Simulated LST Map of Spring 2050

The LST maps of spring 2014 and 2020 are reclassified into 4 classes (0–14 °C; 14–20 °C; 20–24 °C; 24–39 °C) (Table 3). The simulated LST map of the study region of spring 2050 with four categories is shown in Figure 6. From Table 3 and Figure 6, it is observed that the area of the study region falling under the lowest LST category (0–14 °C) is decreasing between 2014 and 2020. This decreasing trend is expected to continue in the future in 2050 with only 0.18 km² remaining in this LST category implying rapid decrease in areas with lowest surface temperature in the study region. It is also observed that 294.72 km² of the study region had LST range between 24–39 °C in 2020 which might increase by six times (1,654.45 km²) in 2050. From this analysis it could be interpreted that the built-up areas and the open lands of the study region which exhibit higher LST between 2014 and 2020 may get hotter in 2050 as the urbanization of the study region increases in the future. It is also to be noted that the simulation result of LST is based only on the historic LST maps of 2014 and 2020 which are considerably hotter and this could also be one of the reasons for the LST maps of 2050 to have major areas of Växjö municipality in the highest LST category (24–39 °C). Thus, it becomes necessary to include the seasonal dataset of the past two decades to study in detail the trend in LST change of the study region.

INFLUENCE OF SEASONAL VARIATIONS OF NDVI AND NDBI ON LST

The seasonal variations in the relationships between LST, NDVI and NDBI during of the study region in 2019 is calculated as shown in Figure 2 and the results are shown in Figure 7 (a)–(c). The results suggest that there is a strong positive correlation between LST and NDBI (0.74) (Figure 7(b)) suggesting that increase in built-up could possibly increase the LST of the study region. Negative correlation between LST and NDVI (-0.65) (Figure 7(a)), NDVI and NDBI (-0.71) (Figure 7(c)) indicates that decrease in vegetation might be one of the factors for the increasing LST in the study region. It is also to be noted that the correlation between LST, NDVI and NDBI is at the maximum during the summer of 2019. Thus, it could be understood that

in the current study region, to study the influence of change in built-up and vegetation on the surface temperature, it is essential to make use of the satellite images of summer. This analysis highlights the fact that the relationships of LST with land cover indices including NDBI, NDVI varies from region to region and also it depends upon the season of the year and time of the day.

Conclusion

In this study, the influence of increasing urban development on the land surface temperature of Växjö Municipality between 2014 and 2020 was studied using Landsat 8 data. Results suggest that the area of observed built-up had doubled between 2014 (28.46 km^2) and 2020 (64.34 km^2) with an increase in mean land surface temperature by 3.8 °C. Cellular Automata based modeling technique was implemented to simulate the urban growth and land surface temperature of the region in 2050. Simulation results indicate that built-up area might quadruple (258.99 km^2) in 2050. Simulated LST map of spring 2050 suggests that the hotter regions (24–39 °C) of 2020 might increase by almost six folds (1,654.45 km^2) in 2050. It is also to be noted that the simulated land surface temperature map of the

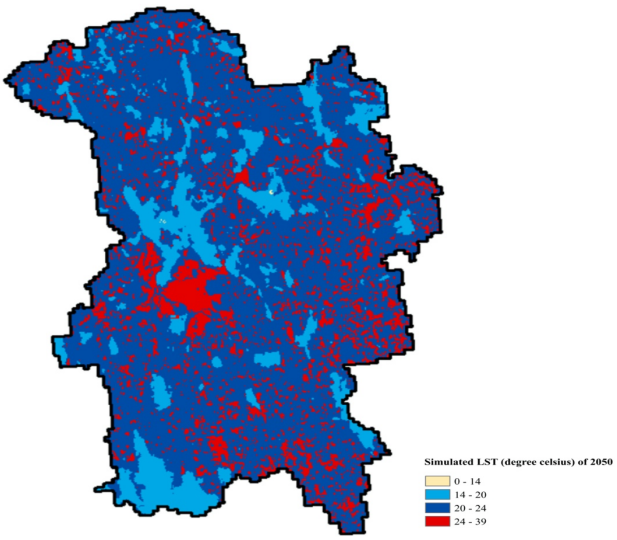

Figure 6. Simulated LST Map of the study region in Spring 2050.

Table 3. Areas of LST categories observed in Spring 2014 and 2020 and expected in Spring 2050.

LST Categories (°C)	Area (sq.km) of LST categories in		
	2014	2020	2050
0–14	1,874.73	5.39	0.18
14–20	51.60	273.53	266.87
20–24	0.35	1,353.36	5.50
24–39	0.32	294.72	1,654.45

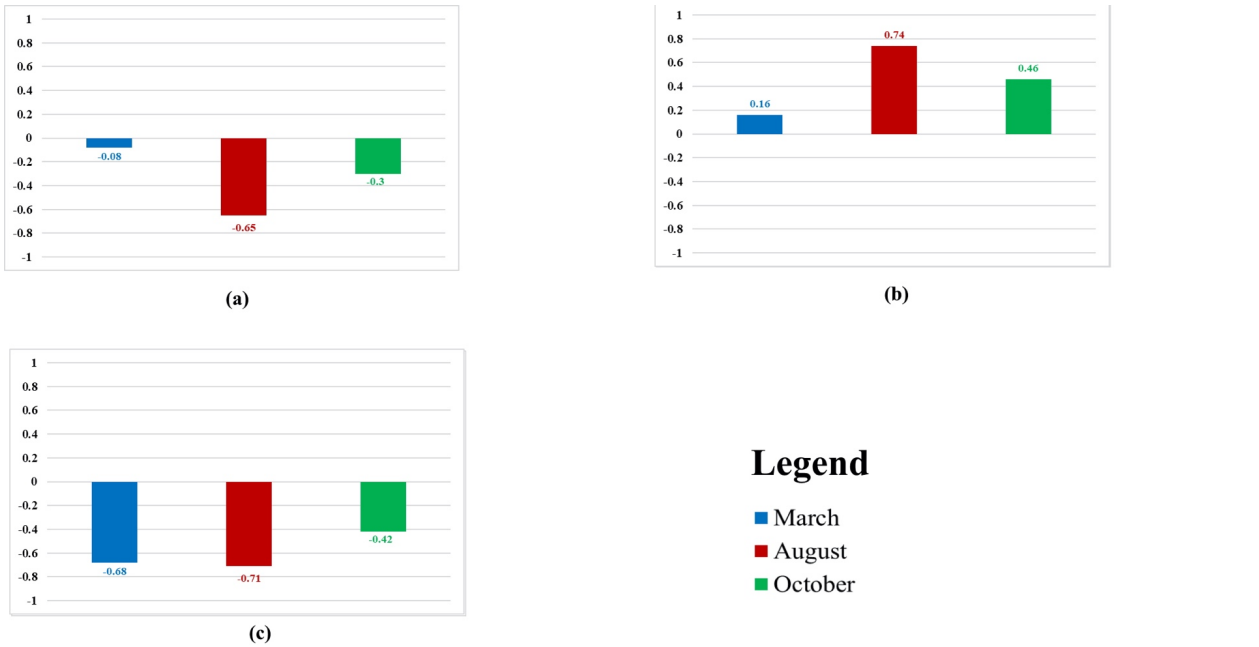

Figure 7. Seasonal variations in the relationship between observed (a) LST and NDVI; (b) LST and NDBI; (c) NDVI and NDBI; of the study region in 2019.

study region of spring 2050 is based only on the LST maps of the spring of 2014 and 2020. A detailed study on considering the LST changes making use of seasonal data of past 20 years is necessary to study the pattern of LST changes in the study region. Further, the analysis on the seasonal variations on the relationship between LST, NDVI and NDBI made use of only the spring, summer, and autumn data of 2019 due to the non-availability of winter dataset of 2019. Hence, for a better understanding of the influence of changes in NDVI and NDBI values on the LST of the study region, it becomes crucial to include all the seasonal datasets in the analysis.

In this study, traditional cellular automata-based model by making use of only the historical urban maps of the region are used in the simulation process. However, when parameters including the population density, transportation network, constraints including areas where urbanization is restricted including areas closer to waterbodies, ecologically sensitive areas and so on, are included in the cellular automata model, the prediction analysis would depict the urban reality with higher accuracy. Further, implementing and validating the cellular automata model along with various factors of urban development for the current time period would enable the futuristic prediction results more reliable. Considering the dual nature of the relationship between land use/land cover and the climate change, the impact of changing climatic conditions on the land cover patterns is to be studied which could provide a better understanding on the interlinkage between climate change and land use/land cover of the region. A thorough study on the urban growth trend and its impact on the increasing surface temperature of the study region with the past two decadal datasets is necessary to provide a clear understanding of the consequences of urban development on the surface temperature of the region. In any case, this study is a step forward in the direction of analyzing the impact of surface temperature on the global climate change due to the urban development patterns which would enable the local governing authorities to devise appropriate urban planning strategies so as to minimize the impact of urban growth on the thermal environment of the municipality.

List of Abbreviations

BT	Brightness Temperature
CA	Cellular Automata
GIS	Geographic Information System
k	Kappa Co-efficient
LST	Land Surface Temperature
NDBI	Normalised Difference Built-Up Index
NDVI	Normalised Difference Vegetation Index
OA	Overall Accuracy
P_v	Proportion of Vegetation
SDG	Sustainable Development Goal
SVM	Support Vector Machine
TOA	Top Of Atmospheric
TPM	Transition Potential Matrix

References

Aarthi, A. D. and Gnanappazham, L. (2018). Urban growth prediction using neural network coupled agents-based Cellular Automata model for Sriperumbudur Taluk, Tamil Nadu, India. *The Egyptian Journal of Remote Sensing and Space Science*, 21 (3): 353–362.

Aburas, M. M., Ho, Y. M., Pradhan, B., Salleh, A. H. and Alazaiza, M. Y. D. (2021). Spatio-temoral simulation of future urban growth trends using an integrated CA-Markov model. *Arabian Journal of Geosciences*, 14: 131. 10.1007/s12517-021-06487-8.

Aik, D. H. J., Ismail, M. H. and Muharam, F. M. (2020). Land Use/Land Cover Changes and the Relationship with Land Surface Temperature Using Landsat and MODIS Imageries in Cameron Highlands, Malaysia. *Land*, 9, 372. 10.3390/land9100372.

Dissanayake, DMSLB., Morimoto, T., Murayama, Y. and Ranagalage, M. (2019). Impact of Landscape Structure on the Variation of Land Surface Temperature in Sub-Saharan Region: A Case Study of Addis Ababa using Landsat Data (1986–2016). *Sustainability*,11, 2257. 10.3390/su11082257.

European Environment Agency (2021). Indicator Assessment: Global and European temperatures. Available from https://www.eea.europa.eu/data-and-maps/indicators/global-and-european-temperature-10/assessment. Accessed on 25 March 2021.

Fang, P., Zhang, X., Wei, P., Wang, Y., Zhang, H., Liu, F. and Zhao, J. (2020). The Classification Performance and Mechanism of Machine Learning Algorithms in Winter Wheat Mapping Using Sentinel-2 10 m Resolution Imagery. *Applied Sciences*, 10, 5075. 10.3390/app10155075.

Govil, H., Guha, S., Diwan, P., Gill, N. and Dey, A. (2020). Analyzing Linear Relationships of LST with NDVI and MNDISI Using Various Resolution Levels of Landsat 8 OLI and TIRS Data. In: N. Sharma, A. Chakrabarti, V. Balas (Eds.). *Data Management, Analytics and Innovation. Advances in Intelligent Systems and Computing*, Vol. 1042, Singapore: Springer.

Guha, S., Govil, H., Dey, A. and Gill, N. (2018). Analytical study of land surface temperature with NDVI and NDBI using Landsat 8 OLI and TIRS data in Florence and Naples city, Italy. *European Journal of Remote Sensing*, 51 (1): 667–678.

Kumar, D. and Shekhar, S. (2015). Statistical analysis of land surface temperature–vegetation indexes relationship through thermal remote sensing. *Ecotoxicology and Environmental Safety*, 121: 39–44.

Li, X. and Gong, P. (2016). Urban growth models: progress and perspective. *Science Bulletin*, 61 (21): 1637–1650.

Mancino, G., Ferrara, A., Padula, A. and Nole, A. (2020). Cross-Comparison between Landsat 8 (OLI) and Landsat 7 (ETM+) Derived Vegetation Indices in a Mediterranean Environment. *Remote Sensing*: 12 (2), 291.

Mathur, A. and Foody, G. M. Land cover classification by support vector machine: towards efficient training. *IEEE International Geoscience and Remote Sensing Symposium*, Anchorage, AK, USA, 2004, pp. 742–744. 10.1109/IGARSS.2004.1368508.

Meng, X., Cheng, J., Zhao, S., Liu, S. and Yao, Y. (2019). Estimating Land Surface Temperature from Landsat-8 Data using the NOAA JPSS Enterprise Algorithm. *Remote Sensing*, 11, 155. 10.3390/rs11020155.

Meyer, W. B. and Turner II, B. L. (Eds.). (1994). *Changes in Land Use and Land Cover: A Global Perspective*. Cambridge, UK: Cambridge University Press.

Mubea, K., Goetzke, R. and Menz, G. (2014). Applying Cellular Automata for Simulating and Assessing Urban Growth Scenario Based in Nairobi, Kenya. *International Journal of Advanced Computer Science and Applications*, 5 (2): 1–13.

Mukherjee, F. and Singh, D. (2020). Assessing Land Use-Land Cover Change and Its Impact on Land Surface Temperature Using LANDSAT Data: A Comparison of Two Urban Areas in India. *Earth Systems and Environment*, 4: 385–407.

Nasehi, S., Namin, A. I. and Salehi, E. (2019). Simulation of land cover changes in urban area using CA-Markov model (case study: zone 2 in Tehran, Iran). *Modeling Earth Systems and Environment*, 5: 193–202.

Ogashawara, I. and Bastos, V. S. B. (2012). A Quantitative Approach for Analyzing the Relationship between Urban Heat Islands and Land Cover. *Remote Sensing*, 4, 3596–3618. 10.3390/rs4113596.

Qiao, Z., Liu, L., Qin, Y., Xu, X., Wang, B. and Liu, Z. (2020). The Impact of Urban Renewal on Land Surface Temperature Changes: A Case Study in the Main City of Guangzhou, China. *Remote Sensing*, 12, 794. 10.3390/rs12050794.

Qin, Z. and Karnieli, A. (2001). A mono-window algorithm for retrieving land surface temperature from Landsat TM data and its application to the Israel-Egypt border region. *International Journal of Remote Sensing*, 22 (18): 3719–3746.

Richards, J. (2013). *Remote Sensing Digital Image Analysis: An Introduction*. Verlag Berlin Heidelberg: Springer.

Rosenfield, G. and Fitzpatrick-Lins, K. (1986). A coefficient of agreement as a measure of thematic classification accuracy. *Photogrammetric Engineering and Remote Sensing*, 52: 223–227.

Shi, D. and Yang, X. (2015). Support Vector Machines for Land Cover Mapping from Remote Sensor Imagery. In: J. Li. & X. Yang (Eds.). *Monitoring and Modeling of Global Changes: A Geomatics Perspective* (pp. 265–320). Springer Remote Sensing/Photogrammetry: Springer, Dordrecht.

Srivastava, P. K., Majumdar, T. J. and Bhattacharya, A. K. (2009). Surface temperature estimation in Singhbhum Shear Zone of India using Landsat-7 ETM+ thermal infrared data. *Advances in Space Research*, 43: 1563–1574.

Sun, L., Chen, J., Li, Q. and Huang, D. (2020). Dramatic uneven urbanization of large cities throughout the world in recent decades. *Nature Communications*, 11: 5366. 10.1038/s41467-020-19158-1.

Tariq, A. and Shu, H. (2020). CA-Markov Chain Analysis of Seasonal Land Surface Temperature and Land Use Land Cover Change Using Optical Multi-Temporal Satellite Data of Faisalabad, Pakistan. *Remote Sensing*, 12, 3402. 10.3390/rs12203402.

Triantakonstantis, D. and Mountrakis, G. (2012). Urban Growth Prediction: A Review of Computational Models and Human Perceptions. *Journal of Geographic Information System*, 4 (6): 555–587.

United Nations, (2018). World Urbanization Prospects. Available from https://population.un.org/wup/. Accessed on 17 March 2021.

Yan, Y., Mao, K., Shi, J., Piao, S., Shen, X., Dozier, J., Liu, Y., Ren, H. and Bao, Q. (2020). Driving forces of land surface temperature anomalous changes in North America in 2002–2018. *Scientific Reports*, 10, 6931. 10.1038/s41598-020-63701-5.

Yang, H., Xi, C., Zhao, X., Mao, P., Wang, Z., Shi, Y., He, T. and Li, Z. (2020). Measuring the Urban Land Surface Temperature Variations Under Zhengzhou City Expansion Using Landsat-Like Data. *Remote Sensing*, 12 (5), 801. 10.3390/rs12050801.